Journal of Cellular Biochemistry 97:916–932 (2006)

In Vivo Photothermal Flow Cytometry: Imaging and Detection of Individual Cells in Blood and Lymph Flow

Vladimir P. Zharov,[1]* Ekaterina I. Galanzha,[1,2] and Valery V. Tuchin[2]

[1]Philips Classic Laser Laboratories, University of Arkansas for Medical Sciences, Little Rock, Arkansas, 72205
[2]Saratov State University, Saratov, Russia 410026

Abstract Flow cytometry is a well-established, powerful technique for studying cells in artificial flow in vitro. This review covers a new potential application of this technique for studying normal and abnormal cells in their native condition in blood or lymph flow in vivo. Specifically, the capabilities of the label-free photothermal (PT) technique for detecting and imaging cells in the microvessel network of rat mesentery are analyzed from the point of view of overcoming the problems of flow cytometry in vivo. These problems include, among others, the influences of light scattering and absorption in vessel walls and surrounding tissues, instability of cell velocity, and cells numbers and positions in a vessel's cross-section. The potential applications of this new approach in cell biochemistry and medicine are discussed, including molecular imaging; studying the metabolism and pathogenesis of many diseases at a cellular level; and monitoring and quantifying metastatic and apoptotic cells, and/or their responses to therapeutic interventions (e.g., drug or radiation), in natural biological environments. J. Cell. Biochem. 97: 916–932, 2006.

Key words: cells; blood and lymph vessels; flow cytometry; gold labels; molecular imaging; photothermal technique; rat mesentery; small animal

Flow cytometry (FC) represents a recent advance that has revolutionized many areas of cell biology and medicine, especially cancer diagnosis and treatment assessment [Givan, 2001]. In conventional FC, cells extracted from a person and labeled ex vivo are introduced into a high-speed (up to 5–20 m/s) laminar flow produced by a hydrodynamic focusing technique. The isolated cells in a linear stream very quickly (up to 10^4–10^5 cells/s) cross an area irradiated with one or more elliptically-focused laser beams, and fluorescent and/or forward and sideways scattering light is recorded with several photodetectors with spectral filters. This technique is widely used in basic and clinical research to provide, among other applications, rapid analysis of large populations of cells; information on cell sizes and shapes; detection of rare cells; and evaluation of drug–cell interactions [Frazer, 2000; Harding et al., 2000]. Image analyzers (e.g., CAS 200, Becton Dickinson Immunocytometry Systems; and ImageStream, Amnis Corp.) have significantly extended the ability of FC to image cells in flow with a reasonable resolution of ~1 μm and a flow velocity up to 5 m/s [Tibbe et al., 2002; Kubota, 2003; George et al., 2004]. These time-resolved techniques provide morphologic analysis of different moving targets in vitro, such as aggregated platelets, and red and white blood cells (RBCs and WBCs) [Tibbe et al., 2002], and include information on cell orientation, velocity, and even acceleration.

Although in vitro FC is a powerful, established diagnostic method, in vivo studies are necessary to assess physiologic and pathologic processes involving cell metabolism and cell–cell interactions (e.g., aggregation, rolling effects, or adhesion and migration through vessel walls) in the real, complex environment

Grant sponsor: NIH/NIBIB; Grant numbers: EB001858, EB-000873; Grant sponsor: NIH/NCI; Grant number: CA097422.

*Correspondence to: Vladimir P. Zharov, 4301 W. Markham St., Little Rock, AR 72205-7199.
E-mail: zharovvladimirp@uams.edu

Received 15 November 2005; Accepted 16 November 2005
DOI 10.1002/jcb.20766

of living organisms. In vivo studies would preclude invasive isolation of cells from their native environment and avoid processing steps that may not only introduce artifacts, but also make it impossible to examine the same cell population over long time periods. Also, detection and quantification of circulating cells in vivo, in their native state, is potentially important for the early diagnosis of many diseases (e.g., cancer, diabetes, cardiac diseases), or for the study of the influence of the different interventions (e.g., drugs, smoking, radiation) on individual cells [Minamitani et al., 2003; Cherry, 2004]. In particular, to understand the mechanism of the development of metastasis, it is important to monitor tumor cell migration and interaction with other cells [Condeelis and Segall, 2003; Yamamoto et al., 2004; Tozer et al., 2005]. And finally, in vivo study of apoptosis with advanced molecular imaging is crucial for understanding human metabolic and immune system function [Brauer, 2003; Jamin et al., 2003].

The potential adaptation of FC from in vitro to in vivo requires many precautions, even though cell velocity in blood, and especially in lymph flow, is much slower (from 0.3–5 mm/s in blood microvessels to 0.2–0.5 m/s in large blood vessels of animals and humans) than the maximum speed of analysis achieved in FC (see above), which from this perspective makes FC's technical platform easy to adapt to an in vivo setting. However, in vivo studies may be limited by (1) poor optical conditions (compared to an almost ideal situation in vitro), such as scattering and absorption of laser radiation by the vessel wall and surrounding tissues (e.g., skin layers, connective tissue, muscles, fat, other tissue components); (2) difficulties of noninvasively accessing deep vessels; (3) problems with the use of a transillumination optical scheme, which is more convenient for achieving high-resolution; and (4) instability of blood- and, especially, lymph-flow parameters (e.g., fluctuation of cell velocity and the positions and numbers of cells in vessel cross-sections) compared to the well-controlled flow parameters of in vitro FC when separated and focused along the flow axis of single cells successively passing the area of detection. These limitations require some precautions in the choices of a detection system and proper animal models as a first step toward transitioning this technique to human applications.

Many noninvasive methods have already been used to visualize single cells in vivo, including positron emission tomography, magnetic resonance imaging, and different modifications of optical microscopy (e.g., laser Doppler optical coherence tomography, speckle interferometry, optical scattering imaging, 4-D elastic light-scattering spectroscopy, and Raman spectroscopy) [Novak et al., 2004; Zharov et al., 2005a and refs. there]. These techniques span a wide range of parameters, and each is suitable for studying different aspects of these complex phenomena. However, none of them is optimal for quantitatively detecting changes in the number of circulating cells or for continuously imaging cells in relatively fast flow. Therefore, a new detection system is required.

Various animal models that were used to study microcirculation using vital optical microscopy (e.g., rabbit or mouse ear, bat's wing, hamster or mouse dorsal skin-flap window or skinfold chamber, hamster cheek pouch, or mouse open cremaster muscle) can be adapted for FC in vivo with some precautions [Zharov et al., 2005a]. In particular, the desire to realize high-resolution imaging of individual flowing cells may be limited by significant light scattering from surrounding tissue (e.g., skin) and/or by the relatively deep location of vessels into the skin (or other tissue), which makes it difficult to use high-magnification objectives (60–100×) with a short focal distance. Furthermore, most of these models are not suitable for studying cells of lymph flow or in vascular structures of lymph nodes because of the low image contrast of the colorless lymphatics or the difficulties of accessing deep lymphatics using conventional optical methods.

To date, the best optical images of both lymph and blood microvessels have been obtained in the mesentery of the frog, mouse, and rat [Zharov et al., 2005a and refs. there]. Of these, the rat represents an excellent mammalian model (with regard to size, physiology, pharmacokinetics, etc.) [Murakami and Kobayashi, 2005] for broadening medical applications, including single-cell diagnostics. The unique advantages of rat mesentery are its very thin (8–17 μm) [Barber et al., 1987], transparent, duplex connective tissue with a single layer of blood and well-developed lymph microvessels that are easy to access. Additionally, there is no notable influence from the preparation procedure on microcirculation or blood cell properties

after at least 5 h [Horstick et al., 2000]. These features make rat mesentery a very attractive model for some applications of in vivo FC. To date, to our knowledge, only a few attempts to develop in vivo FC in an animal model have been relatively successful using fluorescent [Georgakoudi et al., 2004; Novak et al., 2004] and photothermal (PT) techniques [Zharov et al., 2004a, 2005a,b; Galanzha et al., 2005].

FLOW CYTOMETRY IN VIVO WITH FLUORESCENT DETECTION

The use of a confocal microscopic scheme with fluorescent detection allowed characterizing the in vivo kinetics of labeled RBCs, WBCs, and cancer cells circulating in blood microvessels in mouse ear skin at a typical depth of around 50 μm [Georgakoudi et al., 2004; Novak et al., 2004]. In this scheme, fluorescent signals from the cell population of interest were recorded as the cells passed through a slit of He-Ne laser light focused across 20–50-μm blood vessels. Emitted fluorescence was collected by microscope objectives, and directed though a dichroic splitter and mirrors to photomultiplier tubes. RBCs were isolated from the animal, fluorescently labeled ex vivo, and then reinjected into the animal. In contrast, WBCs were labeled in vivo by injecting a WBC surface antigen-specific antibody. It was observed that the number of circulating RBCs remained constant for at least 3 days, while the number of WBCs decreased significantly in a few hours compared to the much longer life of non-labeled cells. This finding resulted from the influence of the tags on genuine cell interactions in flow. These experiments also revealed the dependence of the kinetics of circulating cancer cells, and in particular, the dependence of the rate of cell elimination from blood flow, on the type of cancer cells, and the host environment.

Another issue affecting the status of FC in vivo is the need for an imaging technique that will allow us to obtain successive high-resolution images of individual cells. Vital microscopy, mainly transmission microscopy, has produced images of single cells in selected superficial blood microvessels with reasonable spatial ($\sim$0.8–2 μm) and temporal (10^{-3} s) resolution [Rosenbaum et al., 2002; Kim et al., 2005; Lipowsky, 2005]. However, to date, images of single cells in fast flow ($\sim$1–5 mm/s) are obtained during one short exposure only (i.e., no successive high-speed framing), while continuous imaging (i.e., successive framing) can be realized only in relatively slow flow ($<$0.1 mm/s). For example, very interesting data on the accumulation of fluorescently-labeled cancer cells on blood vessel endothelium has been obtained using the relatively slow frame rate (15–30 fps) of confocal imaging [Sipkins et al., 2005]. It is still a challenge to realize the successive high-resolution imaging of cells in relatively fast ($>$0.5 mm/s) blood and lymph flow, including flow in lymph nodes, which is crucial for studying cellular dynamics (e.g., cell deformability), including time-resolved monitoring of the interaction of metastatic cells with normal cells in flow and in endothelium.

Despite significant progress in developing new labels [Bornhop et al., 2001] (e.g., quantum dots, fluorescent antibodies specific for subtypes of dendritic cells, etc. [Becker et al., 2003]), the very powerful fluorescent-labeling technique currently used in most in vivo experiments (as in many other in vitro experiments using FC techniques) has drawbacks, as it is potentially subject to photobleaching (despite the short exposure time), blinking, or cytotoxicity. Moreover, growing evidence shows that fluorescent labeling may seriously distort genuine cell properties and the physiologic function of target tissues [Nolte et al., 2004]. For example, acridine orange and rhodamine 6G, fluorescent markers for leukocytes, have been demonstrated to be mutagenic and carcinogenic, as well as possibly causing phototoxic effects [Wei et al., 2003 and included references]. Fluorescent imaging of lymphatics by injecting fluorescein isothiocyanate (FITC)–dextran into the interstitial space has led to elevated interstitial pressure and altered lymph viscosity [Zhang et al., 1997]. These facts may cause some concern regarding the kinetics of labeled cells in flow, and in particular, about the main cause of cancer cell accumulation on vessel walls (i.e., whether accumulation is due to actual cell properties or the strong influence of the tags, as in the above case of WBCs). This issue gains importance in in vivo studies in humans.

Compared to single-photon microscopy, multiphoton fluorescent microscopy can partially overcome some of the above-mentioned problems by significantly increasing spatial resolution and the depth of light penetration in microvessels located deeper in tissue, by reducing out-of-focus photodamage and photobleaching. However, in

the focal plane, photodamage and photobleaching can be worse than in single-photon microscopy [Tauer, 2002]. In addition, strong focusing provides a very small area of detection. In the case of relatively large microvessels, this is a disadvantage, as this approach does not provide reliable detection of each labeled cell within the vessel's cross-section. Thus, because the fluorescent technique must be used cautiously in vivo, other approaches without conventional labeling are needed.

FEATURES OF PHOTOTHERMAL SPECTROSCOPY/MICROSCOPY

General Principle

PT-based methods, such as photoacoustic (PA), thermolens, and other similar techniques that do not require conventional labeling and are not sensitive to light scattering, represent possible alternatives for developing FC in vivo. In these methods, light absorption by cellular components, most of which naturally have no or weak fluorescence, is measured by monitoring thermal and related effects taking place directly in cells as a result of non-radiative relaxation of the absorbed energy in heat. For non-fluorescent samples, PT methods with laser sources currently offer the highest sensitivity for the absorption coefficient, on the order of 10^{-5}–10^{-6}/cm [Zharov and Letokhov, 1986], which makes it possible to noninvasively (a short-term temperature elevation $\leq$1–10°C) detect a single, unlabeled biomolecule with a sensitivity comparable with that of laser-fluorescence methods (i.e., with labeling) [Tokeshi et al., 2001]. To date, these methods, and in particular, PA spectroscopy and time-resolved two-beam (pump-probe) PT spectroscopy, have been used successfully in biochemistry to study the kinetics of relaxation processes in biomolecules in solution; photochemical reactions and photosynthesis; spectroscopy of hemoproteins such as oxidized and reduced cytochrome (Cyt) *c*, hemoglobin, and other cellular components; monitoring the redox state of the respiratory chain in liquid and thin-layer chromatography; and other related biochemical applications [Zharov, 1986; Zharov and Letokhov, 1986; Falvey, 1997].

PT imaging (PTI) has demonstrated in vitro the capability of non-invasively visualizing non-fluorescent absorbing cellular structures, at the living single-cell level in suspension or on a substrate that are not visible by other techniques [Zharov and Lapotko, 2005]. In particular, the thermal-lens microscope on a microchip platform has been successfully used to study the redistribution of cellular Cyt *c* during apoptosis [Tamaki et al., 2002], carcinoembryonic antigen (a marker of colon cancer) in human serum [Sato et al., 2001], and immunoglobulin molecules labeled with gold nanoparticles on the surface of RBCs [Kimura et al., 2001]. Another modification of the PT method, via detection of a phase-shift between the two spatially separated beams of an interferometer in frequency-domain mode, has provided high-resolution imaging of 5–80-nm gold nanoparticles for protein detection in cells [Cognet et al., 2003].

PT Scanning Cytometry

The technical platform for PT cell study is microscopy, which allows great flexibility in choosing the regimen of signal acquisition and simplifies cell manipulation. However, to create images, most described techniques require time-consuming scanning of a focused laser beam across the cells. For example, with the PT thermolens technique, cell imaging with a resolution of $\sim$1 μm was achieved by laser scanning of one cell for $\sim$1 h [Tamaki et al., 2002]. In our modification of a wide-field PT cytometer, the PT image from one cell was obtained in 0.1 s after just one laser pulse with an 8-ns width and a broad-beam diameter (15–25 μm) covering entire cells [Zharov and Lapotko, 2005]. With this modification, there is no need for time-consuming conventional scanning with a strongly focused laser beam across the cells, as in the first scheme. However, to obtain PT images from different cells, the laser irradiates one cell; then, the position of the laser beam's center must be moved to another cell and the laser then irradiates this cell, and so on. Discrete changes in the position of the laser beam in PT microscopy takes very little time (0.5–5 s) compared to that for conventional continuous laser scanning (0.5–1 min). PT analysis of many cells ($\geq$1,000), however, may take from 10–15 min to hours, which is not convenient for routine cell study, and requires the flow cytometry mode.

Specificity of PT Spectroscopy

Basic informative parameters provided by laser PT spectroscopy include an absorption coefficient similar to those in conventional

absorption spectroscopy (AS). The difference is that in AS, absorption is measured by monitoring light attenuation during passing of the cells, while in PT spectroscopy, light absorbed into cells is measured directly through thermal phenomena. With the development of PT spectroscopy, the capabilities of AS are significantly improved in terms of absorption sensitivity threshold, spectral resolution, and specificity [Zharov and Letokhov, 1986]. Indeed, even with conventional optical sources (e.g., lamp with filter or monochromator), AS using specific absorption signatures (so-called fingerprints) of biomolecules has the potential for label-free identification of many cellular components, including catalase, peroxidase, flavoproteins (e.g., NADH-dehydrogenase), cytochromes (P450, b_5, a, c, c_1, b), cytochrome-c oxidase, and others [Jacobs and Worwood, 1974].

Most of these components have distinctive, relatively narrow (10–30 nm), isolated spectral bands in the visible and near-infrared (IR) spectral range of 400–900 nm, without the significant influence of DNA, RNA, lipids, and water, which absorb mainly in ultraviolet (<350 nm) and IR (>1,000 nm) ranges. In particular, in the spectral range of 400–900 nm, the lowest absorption background is determined by water (absorption coefficient, 5×10^{-4}–5×10^{-3}/cm), with a further increase in the near-IR range ($\sim 2 \times 10^{-1}$/cm at 1 μm) [Zharov and Letokhov, 1986]. In contrast, most cellular chromophores have much stronger local absorption in the visible and near-IR ranges (on the order of 10^{-1}–10^{2}/cm) [Jacobs and Worwood, 1974]. For example, AS has been successfully used to measure changes in the redox state of Cyt c in mitochondria and to identify cellular Cyt-c oxidase in vivo [Jacobs and Worwood, 1974]. Even in the IR range in the presence of a strong absorption background from water and proteins, AS has the potential to distinguish healthy from cancerous cells, as well as normal cells with different metabolic activities, or apoptotic cells having the spectral signatures of DNA, RNA, and phospholipids [Lasch et al., 2004].

These features of AC provide many successful applications; however, a high concentration of cells in suspension (data on the use of a cell monolayer are scant) is required because of the relatively low absorption sensitivity due to the short optical path of light (L) in cellular micro- and nanostructures (a limitation of AS) [Zharov and Letokhov, 1986]. For example, to measure absorption in a 300-nm-long optical path (the typical diameter of an elongated mitochondrion) with an accuracy of ~0.5% in measuring light variation, a minimum detectable coefficient of absorption (α_{min}) $\approx 1.5 \times 10^{2}$/cm. This level is insufficient for studying cellular structures that typically have a lower coefficient of absorption (see above). Furthermore, in most forms of AS, only the average absorption within whole cells is measured, which prevents spectral identification of localized cellular components.

PT schematics with laser sources provide absorption sensitivities at least four to five orders of magnitude higher than with conventional AS, as well as the capability of measuring localized absorption spectra at the subcellular level with tunable lasers with a spectral width in the range 0.1–1 nm. In particular, PT spectral identification of just three main cellular components, such as cytochrome c, P450, and cytochrome-c oxidase, with distinguishable absorption bands near 450 nm, 550 nm, and 700–900 nm [Jacobs and Worwood, 1974], respectively, may provide many potential applications of PT spectroscopy in biochemistry, as these components are involved in such important cellular processes as apoptosis, drug kinetics, and cellular energy, respectively. The tunable laser in visible and near-IR spectral ranges provides the opportunity to identify additional cellular components such as Cyt a (605 nm) and Cyt-c oxidase with the copper A center (Cu_A) in reduced (620 nm) and oxidized (820 nm) states, and with the copper B center (Cu_B) in oxidized (680 nm) and reduced (760 nm) states. Measurement of PT responses from oxidized (760 nm) and reduced (900–950 nm) hemoglobin may make it possible to estimate the oxidization of RBCs in flow at the single-cell level. Additionally, using specific absorption bands for RBCs (420–430 nm, 580 nm, and 760 nm) and WBCs (550 nm and 800–820 nm), the presence of rare RBCs among WBCs in lymph flow can be identified, as can the presence of rare WBCs among RBCs in blood flow. To identify abnormal cells that do not differ significantly in absorption (e.g., "rigid" RBCs among "flexible" RBCs, or cancer cells among normal WBCs), the correlations between specific PT parameters (i.e., PT-image parameters related to cell shape and structural parameters at specific delay times or PT-response amplitude, shape, and duration) and the morphologic cell

type can be analyzed, in particular, to distinguish small variations in PT-image structures.

INTEGRATED PHOTOTHERMAL FLOW CYTOMETRY IN VIVO

Given the limitations of current imaging systems as described above, a new imaging technique is required. The following describes the proposed use of integrated PTFC for in vivo visualization that is not possible with current systems or techniques.

Schematics

The general schematics integrated multispectral in vivo FC combines basic principles of in vitro FC with recent attempts at in vivo FC [Novak et al., 2004; Zharov et al., 2005a] (Fig. 1). Cell detection occurs in superficial microvessels in the skin or in thin, relatively transparent living biostructures that allow measurement of light transmitted through the vessels. To illuminate selected vessels, different optical sources can be used, ranging from a conventional lamp with filters to lasers in pulsed- or continuous-wave mode. Light beams are focused on a small area of the microvessels (the analysis point). To detect all cells in a cross-section of vessel, the laser beam diameter must cover whole vessel, or at least must illuminate a localized vessel area through which most cells move in the flow stream (e.g., near the axis in an area close to lymphatic valves). To minimize simultaneous irradiation of several cells along the vessel axis, the beam may have an elongated ellipsoidal shape-oriented perpendicular to the vessel axis.

Optical absorption by non-fluorescent cellular structures can be measured with PT and PA methods. Specifically, a PT deflection module with a position-sensitive photodetector is incorporated to measure bioflow velocity (PT velocimetry [Zharov et al., 2004a]), a PT thermolens module to measure integrated time-resolved PT

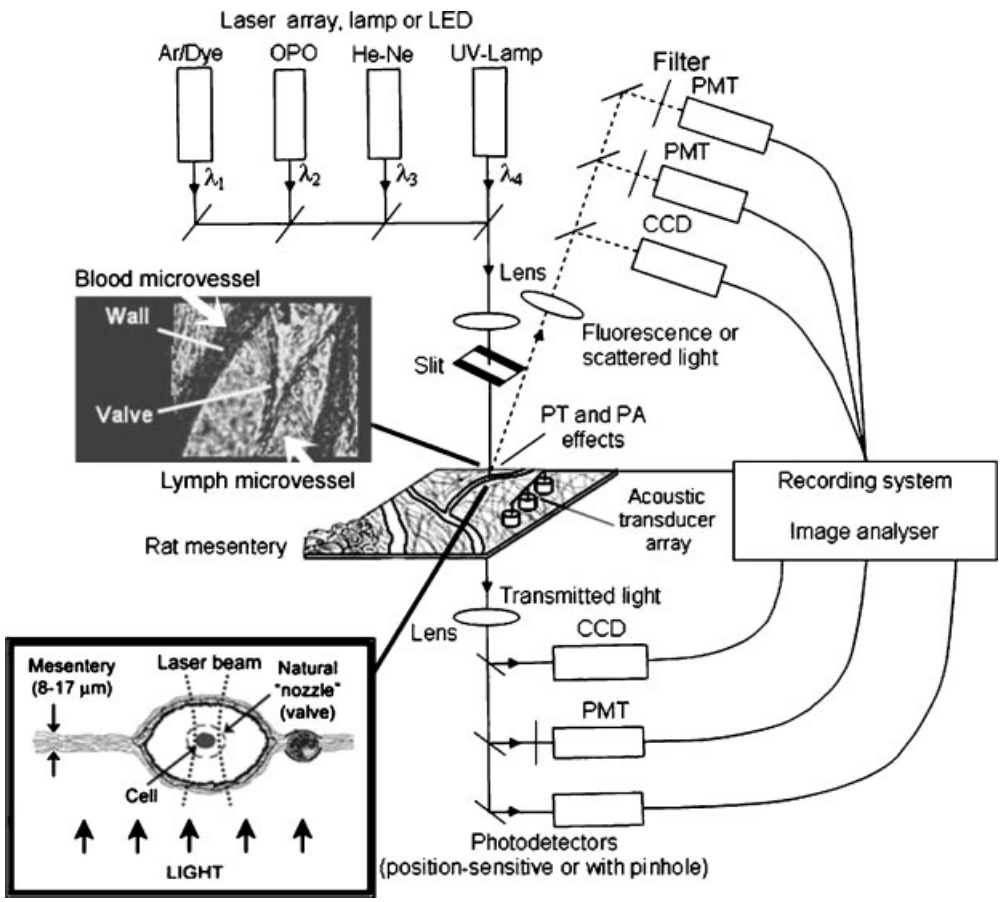

Fig. 1. Schematic of integrated multispectral flow cytometer in vivo combining photothermal, transmission, and fluorescence techniques.

responses from moving cells [Zharov and Lapotko, 2005], and a PTI module to image moving cells alone or with PT labels (e.g., gold nanoparticles) in combination with a thermolens or phase-contrast imaging technique [Zharov and Lapotko, 2005]. Also, a PA transducer or transducer array allows measurement of PA signals from single cells, either alone or with gold labels, in flow with focused laser beams, as well as measurement of PA signals from cells accumulated at specific sites (vessel wall, surrounding tissue, or specific organ) with a relatively broad laser beam using PA tomography schematics [Oraevsky and Karabutov, 2003].

In PTI mode, a single cell or cells are irradiated with a short, focused pump laser pulse (tunable optical parametric oscillator [OPO] laser; wavelength, 415–2,300 nm; pulse width, 8 ns; pulse energy, 10^{-8}–10^{-3} J; Lotis Ltd., Minsk, Belarus). This irradiation leads to an increase in the temperature of local non- or weakly-fluorescent cellular absorbing structures. In turn, temperature distribution is transformed into refraction distribution. Time-resolved monitoring of temperature-dependent variations in the cell's refractive index is realized with thermolens or phase-contrast imaging (technical platform: Olympus BX51 microscope with a CCD camera; AE-260E, Apogee, Inc.) using a second, collinear laser pulse (Raman shifter; wavelength, 639 nm; pulse width, 13 ns; pulse energy, 2 nJ; Fig. 1) [Zharov and Lapotko, 2005]. Special phase microobjectives (20× and 60×) with Zernike coaxial quarter-wave spots with a transmission of 30% and a diameter of 0.7 mm were used to provide phase-contrast imaging of the probe laser beam. The diameters of the pump- and probe-beam spots were 15–20 μm and 10–15 μm, respectively. As a result, formation of a PT image required just one pump pulse with a relatively broad beam-diameter covering entire single cells. Hence, time-consuming scanning with a strongly-focused laser beam across each individual cell, as in conventional laser imaging, was unnecessary. The entire PT image-acquisition procedure includes illumination of a cell with three pulses: an initial probe pulse followed by the pump pulse and then a second probe pulse, with a tunable delay with respect to the pump pulse (0–5,000 ns). The PT image was calculated as the difference between the two probe images) [Zharov and Lapotko, 2005], and depended only on absorption contrast rather than on possible phase distortion of the probe beam itself or natural refractive cellular heterogeneities. This technique allows the capture of PT images of single moving cells with a time delay between laser pulses that is adjustable to cell speed.

A second mode, the thermolens mode, made it possible to record a whole cell's time-resolved integral PT response. In this mode, a pump laser-induced refractive heterogeneity (called a thermolens effect) caused defocusing of a collinear He-Ne laser probe beam (wavelength, 633 nm; power, 1.4 mW), and hence, a reduction in the beam's intensity at its center as detected by a photodiode (C5658; Hamamatsu Corp.) supplied with a 0.5-mm diameter pinhole. The PT response was recorded with a Tektronix TDS 3032B oscilloscope.

The PT-response amplitude and temporal shape depend on several cellular parameters, such as local coefficient absorption, characteristic relaxation times, thermodynamics, and morphological cell properties. In pulse mode, the PT response demonstrates a high initial peak due to fast (nanosecond scale) heating of the absorbing structure, and a much longer (microsecond scale) exponential tail corresponding to the cooling of the cell as a whole.

Because of the laser beam's relatively wide breadth, optical resolution was determined by the microscope objective itself (e.g., ~0.7 μm at 20×, numerical aperture [NA] 0.4; and ~300 nm at 60×, NA 1.25), without significant influence of thermal blurring of the diffraction spot during the short pump pulse.

Because PT methods are relatively new in biological studies, fluorescent techniques (widely used in conventional in vitro FC), together with transmission digital microscopy (TDM), are employed to verify PT data using two additional digital cameras: (a) a sensitive CCD camera with a reasonably fast frame speed (up to 300 fps; Cascade: 650; Photometrics) to image relatively slow-moving WBCs in blood (e.g., rolling leukocytes) and lymph flow; and (b) a high-speed CMOS camera with reasonable sensitivity and a fast frame speed (model MV-D1024-160-CL8, Photon Focus, Switzerland; 2,500 fps for an area 128×256 pixels, and 10,000 fps for 128×64 pixels) sufficient to image strongly absorbing fast-moving RBCs.

The threshold for absorption coefficients is on the order of 10^{-2}–10^{-3}/cm, which is sufficient to

detect most intracellular absorbing structures with a typical local absorption coefficient of 10^{-1}–10^{3}/cm in the visible spectral range. This sensitivity threshold corresponds to laser-induced temperature variations of $\sim 10^{-2}$°C–10°C in a cell. Thus, the temperature fluctuation is small enough not to damage cell structures, especially during the short time of irradiation while cells cross the illuminated area.

HIGH-RESOLTION IMAGING OF FLOWING CELLS

As described above, rat mesentery is the one of the most attractive models for proof of concept of in vivo FC. Rats were narcotized, and the mesentery was exposed and placed on a heated (37.7°C) stage bathed in warm Ringer's solution (37°C, pH 7.4). At different magnifications (4–100×), TDM revealed that the rat mesentery provides a unique opportunity to simultaneously study blood and microlymphatic systems, together with neighboring lymph nodes (Fig. 2) [Zharov et al., 2005a,b; Galanzha et al., 2005]. Indeed, rat mesentery contains a blood microvessel network that includes arterioles (diameter, 7–60 μm; velocity, 5–10 mm/s), venules (10–70 μm; 0.5–3 mm/s), and capillaries (5–9 μm; 0.1–1.4 mm/s), as well as well-developed microlymphatic vessels (diameter, 50–250 μm; velocity, 0–4 mm/s), and clearly distinguishable initial lymphatics with migrating cells (Fig. 2c,d). Some blood microvessels are located very close to lymph microvessels (Fig. 2e) and the parallel geometry of these vessels makes it possible to study cell migration between the two systems.

This model was able to provide in vivo imaging of lymph nodes close to mesenteric structures with high optical resolution (~300 nm), with a clearly distinguished vascular network and migrating individual cells (Fig. 2a,b). This technique may make it possible to monitor the migration of the different cells by their typical pathways: blood microvessel (Fig. 2g,h) → tissue interstitium → initial lymphatic (Fig. 2c,d) → afferent lymphatic (Fig. 2e,f) → regional lymph node (Fig. 2a,b). High-resolution TDM allowed us to determine the morphological types of individual cells through visualization of cell shape and size (for example, parachute-like RBCs (Fig. 2i,j), single platelets (Fig. 2h), and

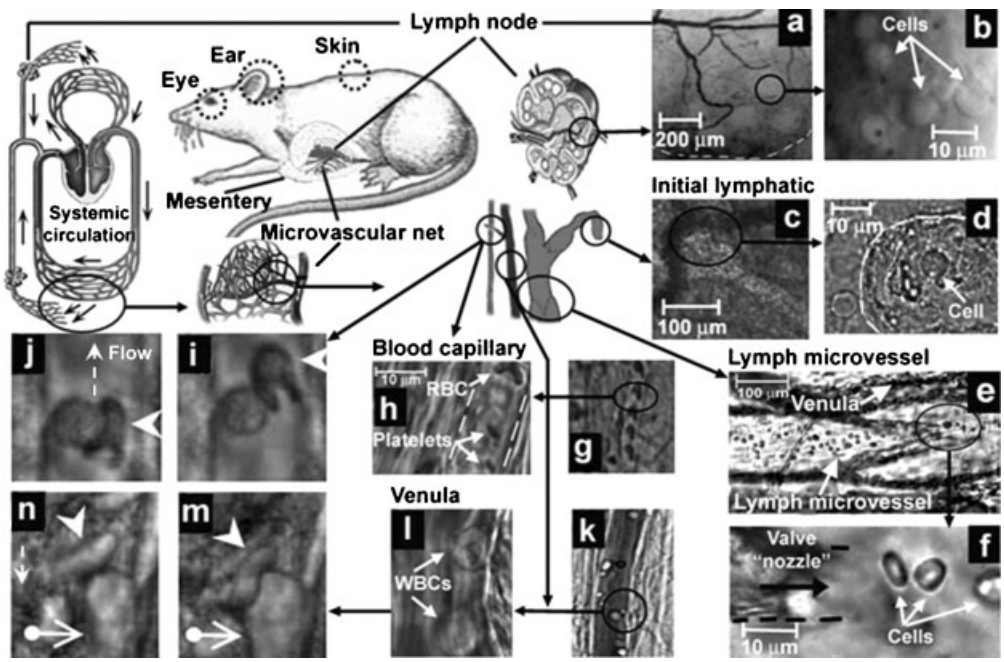

Fig. 2. TDM images of rat mesentery in vivo. **a**, **b**: Fragment of single lymph node with different magnifications (4× and 100×, respectively); **c**, **d**: initial lymphatic (4× and 100×); **e**: lymph vessel with valve and surrounding blood vessels (10×); **f**: valve tip with fast-flowing cells (100×); **g**: capillary with parachute-like RBCs (10×); **h**: platelets in a blood capillary (100×); **i**, **j**: high-speed images of RBCs flowing through narrow slit in blood capillary; **k**, **l**: rolling leukocytes in blood vessels (10×, 100×); and **m**, **n**: interaction of RBC (arrowhead) with rolling leukocytes (arrow with circle).

rolling leukocytes (Fig. 2k,l). In selected experiments, we obtained images (not shown) of subcutaneous blood microvessels through a dorsal skin-flap window and in ear; and we also have the potential to study retinal microvessels of the eye. Despite the relatively low resolution of these images compared to that of images of the mesentery, this achievement potentially allows the simultaneous monitoring of labeled circulating cells in different parts of the rat's body (e.g., shown by dashed circles in the drawing of the rat in Figure 2). Image contrast of these microvessels can be potentially improved by the application of so-called clearing agents) [Tuchin, 2005].

A conventional, low-speed CCD camera (15–25 fps) could image relatively slow-moving migrating cells, rolling leukocytes in blood flow (typical velocity in the range of 30–70 μm/s in venules), and WBCs in small lymphatics (<0.2 mm/s), but a high-speed camera is required to image, without motion distortion, relatively fast-moving RBCs in blood flow (2–10 mm/s in arterioles and large venules) and WBCs in large lymphatic vessels (1–3 mm/s). With a high-speed CMOS camera, we were able to capture successive high-resolution (300 nm) cell images with a very short time period (0.1–1 ms) between frames. In particular, this technique revealed the high deformability of parachute-like RBCs as they squeezed (at 0.4 mm/s) through a narrow gap between the vessel wall and another, rigid RBC adherent to the opposite wall (Fig. 2i,j). It also showed how quickly relatively fast-flowing RBCs (~1 mm/s) changed shape as they interacted with much more slowly moving (rolling) leukocytes (≤50 μm/s) (Fig. 2m,n). We also observed significant dynamic deformation of two RBCs in merging flow streams at a bifurcation zone and extremely fast stretching (0.4 ms at 2,500 fps) of initially discoid RBCs to ~0.7–0.9 μm (not shown). To our knowledge, this was the first time these phenomena have been observed with high-speed, high-resolution imaging in vivo. This technique may permit the study of the dynamics of cell deformability in vivo, including early diagnosis of diseases accompanied by changes in cell deformability (e.g., sickling diseases, anemia, cardiovascular pathologies) [Guck et al., 2005].

TDM's high spatial resolution (up to 300 nm at 100× magnification with water immersion) make it possible to estimate cell size and shape. The low absorption sensitivity of TDM, however, makes it impossible to differentiate individual cells with slight differences in absorption in fast flow in vivo.

In contrast to TDM's low absorption sensitivity, the PT technique is able to not only monitor small variations in absorption in cells as a whole, but also to identify cells on the basis of different PT-image structures associated with specific localized concentrations or the spatial distribution of absorbing biomolecules. In the presence of gaps between neighboring cells in flow (typical for small blood vessels and lymphatics), we used a circular laser-beam geometry. At short distances and, especially, with many overlapping cells, selected experiments in the thermolens mode were performed with an ellipsoidal beam shape. To exclude distortion of high-resolution images due to spatial fluctuation of cells flowing in a cross-section of vessels, especially in relatively large lymphatic vessels (up to 50 μm in 150-μm-diameter lymph vessels), cells were imaged immediately after passing through a lymph valve (which provided a natural type of hydrodynamic focusing) to limit the fluctuation of cells to within a few micrometers (Fig. 2e,f). With such focusing, we obtained good-quality images (similar to images obtained under static conditions) of single cells in lymph flow, such as WBCs, RBCs, and leukemic cells (K562) (Fig. 3). PTI revealed specific absorbing cellular structures (Fig. 3b,e,h) associated with the spatial distribution of cytochromes in WBCs and cancer cells, and hemoglobin in RBCs, that are not visible with TDM (Fig. 3a,d,g, respectively). Fluorescent images obtained with a high-sensitivity CCD camera showed good image contrast (Fig. 3c,f,i) similar to that of PT images, but required inconvenient staining procedures: rhodamine 6G by intravenous injection for WBCs and in vitro labeling with FITC for RBCs and MitoTracker Red for K562 cells, both by intravenous bolus injection. It is noteworthy that the PT techniques are not sensitive to scattering light.

The rotation of single cells in blood and, especially, in lymph flow, can often be observed. This effect opens the way to realizing projection tomography in vivo whereby 2D cell images captured at different angles are reconstructed into 3D cell images using well-developed mathematical algorithms.

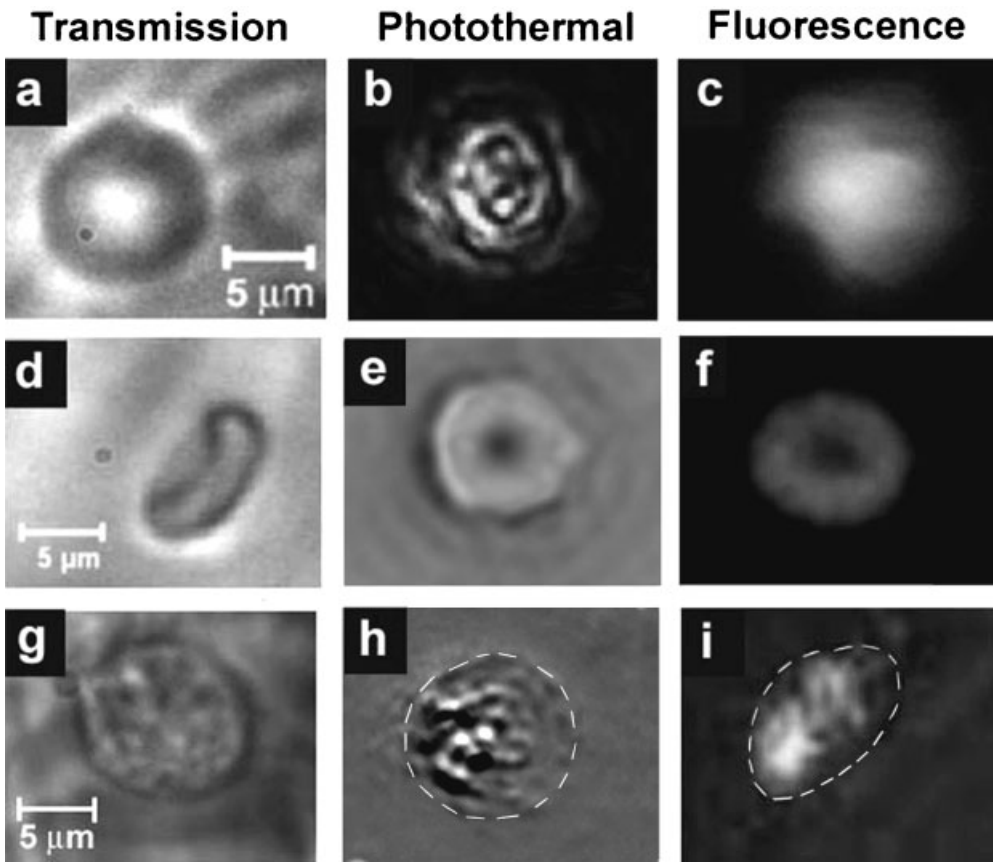

Fig. 3. Transmission (**a**, **d**, **g**), PT (**b**, **e**, **h**), and fluorescent (**c**, **f**, **i**) images of WBC (**top row**), discoid RBC (**middle row**), and cancer cell (K562) (**bottom row**) in flow in vivo.

PT MONITORING OF FLOWING CELLS

With the thermolens mode, continuous PT monitoring of moving blood cells can be realized [Zharov et al., 2005a]. Figure 4, left, a–c shows typical PT-signal tracings from cells as a function of the length of time that it takes for the cell to flow through the irradiation area. PT signals from RBCs in flow showing a purely positive component (Fig. 4, left, a) indicated a standard linear PT response from the cells at a low laser-energy level. The amplitude differences indicated differences in average absorption and reflected RBCs' natural heterogeneity. Figure 4, left, b shows the detection of single RBC at a low laser-energy level that did not produce notable PT signals from many of the WBCs in lymph flow because of their low absorption. Laser-induced vessel injury led to a fast-growing number of RBCs in lymph flow (Fig. 4, left, c). The next tracing shows that the PT signals from RBCs at a relatively high laser-energy level led to cell damage (Fig. 4, left, d). The presence of only a negative PT signal indicated the development of strong, dominant nonlinear effects (e.g., microbubble formation around strongly absorbing cellular zones). The presence of both positive and negative components in the PT-signal amplitude tracing (Fig. 4, left, e) indicated a noninvasive condition for WBCs (which have a high photodamage threshold) and an invasive condition for RBCs (which have a low photodamage threshold) at the same energy level. We used a relatively high laser energy level and a relatively slow oscilloscope rate to demonstrate the capability of PTFC to distinguish cells with different photodamage thresholds. Because of potential differences in the optical properties of normal and cancerous cells, especially mitochondrial distribution, which can be visualized with PTI [Gourley et al., 2005], we could assume that PTFC also had the potential to distinguish these cells.

Modeling of PTFC was also performed in vitro with cell flow realized with a syringe pump-driven system (KD Scientific, Inc.) and glass

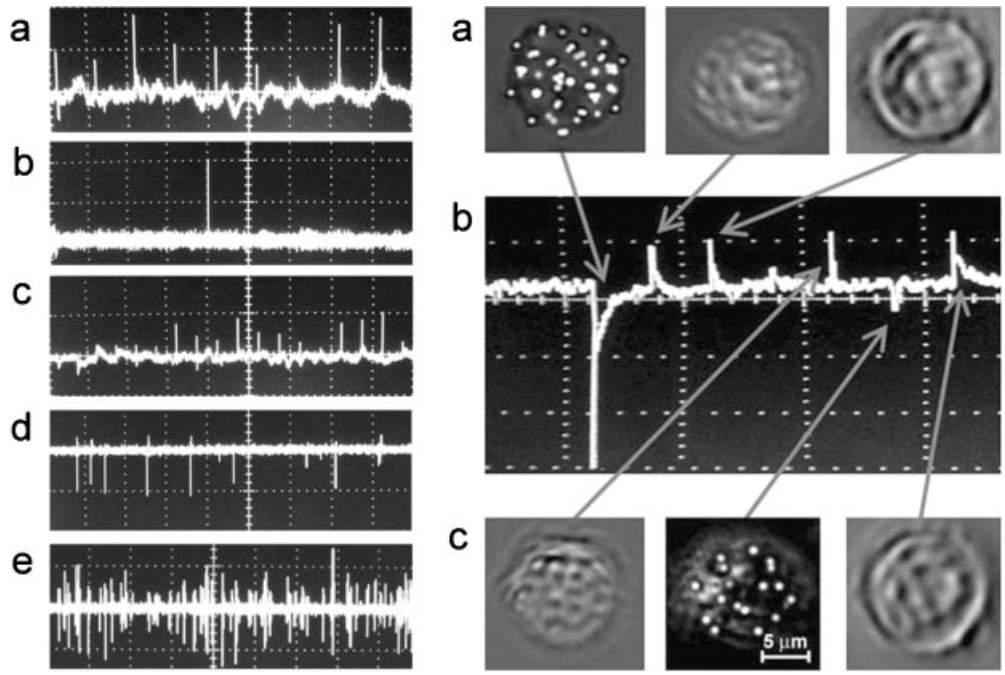

Fig. 4. **Left**: Typical tracings of PT signal from blood cells in blood and lymph flow. **a:** RBCs in blood flow; **b:** rare RBC in lymph flow under normal conditions; **c:** growing number of RBCs in lymph flow during laser-induced hemorrhage; **d:** laser-induced damage of RBCs in lymph flow. **e:** WBCs and RBCs in lymph flow. **Top–bottom**: Laser (λ_P, 525) energy/amplitude/time scale/division: 0.3 μJ/50 mV/100 ms, 0.5 μJ/20 mV/1 s/div, 0.6 μJ/100 mV/200 ms/div, 5 μJ/500 mV/4 s/div, and 145 μJ/100 mV/10 s, respectively. **Right.** PT identification of K562 cells labeled with 40-nm gold nanoparticles in flow. **a** and **c**: PT images. **b:** PT-response amplitude tracings (*arrows*) (time scale on horizontal axis, 200 ms/div). Laser parameters: wavelength, 525 nm; pulse width, 8 ns; laser energy, 35 μJ.

tubes with circular geometry ($D_{inside} = 10–50$ μm). This system provided flow velocities in the range of 0.001 μl/h–147 ml/min, corresponding to a linear velocity of ~3.5 μm/s–~10 m/s in a 100-μm-diameter tube. With this system, we found no notable change in the classic (heating–cooling phenomena) PT-response amplitude and shape at flow velocities up to 0.05 m/s; with a further increase in the flow velocity to 0.1 m/s, a small fluctuation in the PT-response tail appeared, with more profound distortion developing at a flow rate of 2 m/s. However, no significant change in the maximum PT-response amplitude was observed even at the highest flow velocity, 10–20 m/s. We also obtained PT images of RBCs at high flow velocities (up to 2–10 m/s) without notable motion distortion.

PT IDENTIFICATION OF CELLS

Identification of blood cells using the PT technique can be based on differences in the amplitude of the integral PT responses, which are proportional to the cells' average absorption (which is significantly different [~30–40 fold] for RBCs and WBCs) [Zharov et al., 2005a]. PT-image structures related to the specific distribution of cellular chromophores can also be used to determine cell type (e.g., RBCs with relatively smooth distribution of hemoglobin, or WBCs with localized distribution of cytochromes or other absorbing biomolecules). In addition, cells can be roughly identified through differences in PT relaxation (i.e., cooling) times (e.g., 6–10 μs for RBCs with an average size of 5–6 μm, and 20–25 μs for 7–8 μm WBCs) [Zharov et al., 2005a]. Furthermore, the PT amplitude from interstitial absorbing backgrounds in the linear (i.e., noninvasive) mode was ~30–50-fold lower than that from RBCs, which could be explained by the low level of absorption by connective tissue and thin vessel walls. Surprisingly, even for low-absorbing lymphocytes, the corresponding difference in amplitude was lower (~5–10-fold), but still noticeable [Zharov et al., 2005a].

CELL TARGETING WITH GOLD PT LABELS

PT identification of cells with similar absorption properties and sizes, such as subpopulations

of WBCs, may pose a problem. The high absorption sensitivity of the PT technique offers an opportunity to consider gold nanoparticles as a new type of PT label [Zharov et al., 2005d]. These particles have unique properties for studying cells, especially in vivo; they are strong absorbers (four to six orders of magnitude greater than any conventional fluorescent label), which makes it possible to detect single particles even as small as 2 nm. In addition, they are nontoxic, biocompatible, and photostable (i.e., absence of photobleaching or blinking); have a fast thermal response time (up to 10^{-12} s); and can easily be conjugated with proteins and antibodies to label many specific cellular markers. Additionally, they may have adjustable absorption properties in the spectral range of 0.5–1 μm, providing high image contrast for their reliable detection against the absorbing cellular background from water, DNA, and lipids [Zharov et al., 2005d]. When closely located or during aggregation, gold nanoclusters demonstrate red-shift effects; this allows gold nanoparticles, in combination with the PT technique, to be used for aggregation immunoassay at the single-cell level [Zharov et al., 2005d]. The absorption bands of gold nanospheres and nanorods, with adjustable spectral properties, are 60–100 nm and 30–50 nm, respectively. These are not as narrow as in fluorescent probes (e.g., quantum dots), but they should be sufficient for spectral identification.

Gold-labeling procedures may be used as the basis for molecular imaging or laser thermal therapy of cancer cells or infections. For example, the WTY-6 subpopulation of the MDA-MB-231 human breast adenocarcinoma cell line was engineered to express separase, a clustered cell-surface protein [Zharov et al., 2005d], which was targeted with a primary F19 monoclonal antibody (Ab). Goat anti-mouse immunoglobulin G (H + L) conjugated with 40-nm gold nanoparticles was used as a secondary Ab to selectively target the primary Ab. The specific distribution of gold labels attached to separase and, especially, the formation of gold nanoclusters, were observed in parallel with TEM and PTI. This highly specific labeling, which targeted chosen cancer markers, was used to demonstrate selective killing of these cells by laser-induced bubble formation around the gold nanoparticles.

The high sensitivity of PT responses to positions of closely located nanoparticles opens the way for precise PT monitoring of nanoscale distances between nanoparticles, with expected nanometer-scale accuracy. Indeed, with PT spectroscopy, the spectral plasmon resonance shift potentially allows us to monitor, within individuals cells, the average distances between gold (or other metals) nanoparticles in the range of 5–50 nm, with the particle size ranging from 2 nm (which is the current sensitivity threshold of the PT technique) and higher. Potential applications may include measurement of protein–protein interactions; spatial relocation of gold nanoparticles during cell metabolism; cellular dynamics, such as the movement of cell organelles; or response to external stimuli, such as the administration of drugs or radiation. In particular, because the spectral shift depends on the properties of the tissue that surrounds the particle, laser-induced cell coagulation in therapeutic applications may be detected through corresponding spectral shifts.

The PTFC mode may allow PT monitoring with high-temporal and high-spatial resolution of circulating labeled cells in blood and lymph flow, with quantitation of their time-dependent numbers, analogous to fluorescent techniques. The conjugation of gold labels with Abs may potentially affect cell–cell interaction or the elimination rate of labeled cells from blood flow due to Ab-enhanced immune response. To exclude (or estimate) these effects, non-specific gold labeling may be realized with non-conjugated gold particles through conventional endocytosis. It is expected that the few gold particles tagged to a cell and detectable with PTFC do not significantly influence cell-adhesive properties, which is crucial to understanding the genuine interaction of abnormal cells with normal cells in flow and in endothelium. This relatively simple procedure may provide reliable identification of labeled cells in flow. In particular, the PT responses from cells with these gold PT labels show specific negative peaks in nonlinear PT responses (associated with microbubble formation around overheated particles) compared to the positive amplitude peaks of linear PT responses from non-labeled cells at the same laser energy level (Fig. 4, right) [Zharov et al., 2005d]. Simultaneous monitoring of PT images from the same cells confirmed that cells tagged with gold PT labels (Fig. 4 right: a, left; c, center) have specific, highly localized image contrast compared with cell PT images, showing the

relatively smooth contrast of endogenous absorbing structures (Fig. 4 right: a, center and right; c, left and right). We believe that this technique makes it possible to identify labeled metastatic or apoptotic cells circulating in blood and lymphatic flow.

OTHER POTENTIAL APPLICATIONS IN VIVO AND IN VITRO

PT Monitoring of Cell Metabolic Changes, Apoptosis, and Necrosis Under the Impact of Nicotine and Drugs

The biological basis for using PT assays to monitor cell responses to different environmental and therapeutic impacts can briefly be described as follows. Laser radiation initially interacts with endogenous cluster-forming nanoscale absorbers (i.e., absorbing cellular biomolecules, such as Cyt *c*, P450, and others) [Zharov et al., 2005c]. Because of the proximity of nanoabsorbers in these clusters, laser-induced optical, thermal, acoustic, and microbubble-formation phenomena around individual nanoabsorbers may overlap to create linear and nonlinear effects. These effects are extremely sensitive to the spatial reorganization of these nanoabsorbers (biomolecules), which are involved in many cellular signaling pathways associated with cell metabolism, apoptosis, or therapeutic interventions.

From a diagnostic perspective, most chromophores provide the strongest localized absorption in the visible and near-IR regions (at least 10^3–10^4 times higher than background absorption from water, lipids, or DNA). The PT response amplitude and temporal shape depend on several cellular parameters, such as biomolecular concentration and their spatial distribution, local absorption coefficient (e.g., depending on the redox state), characteristic relaxation times, and local thermodynamic and morphological cell properties. Metabolic changes, as well as apoptosis and necrosis, may be accompanied by changes in the properties of localized absorbing structures, and these changes influence the local amplitude on PT images in a linear mode or the integral PT response and response shape in linear and nonlinear modes. For example, shrinkage of absorbing clusters (e.g., whole cells or their organelles) is usually related to apoptosis, whereas swelling phenomena usually develop in the presence of lethal drug doses or necrosis. Spatial relocation of Cyt *c* may be related to its release by mitochondria during apoptosis [Tamaki et al., 2002; Zharov et al., 2005c].

The PT scanning cytometer demonstrated extremely high sensitivity to the response of cells to drugs, nicotine, oxidative stress, and chemicals [Zharov et al., 2004b]. In particular, in addition to being able to detect with high sensitivity (three orders of magnitude better than conventional assays) the impact of low doses of nicotine that are typically present in the blood of smokers, PTI also has the potential to distinguish between the various functional states of normal and cancer cells associated with nicotine-induced apoptotic and necrotic phenomena [Zharov et al., 2005c].

PT assay has the capability for rapid and highly sensitive detection of individual cell responses to the impact of antitumor drugs. Specifically, this technique was used to measure distinctive changes in specific non-linear PT responses after exposure of KB-3 carcinoma cells to the antitumor drug vinblastine in the broad concentration range of 10^{-10} nM–300 nM [Zharov et al., 2004b]. Using existing assays (MTT reduction assay, caspase-3 activation, Cyt-*c* release, poly(ADP-ribose) polymerase cleavage (PARP), and cell- and mitochondrion-size monitoring), it was verified that changes in PT parameters were associated with metabolic changes at low concentrations, increased toxicity-related effects with increased drug concentrations, and the appearance of apoptotic effects at high concentration ranges. PT assay has shown the ability to obtain quantitative data (e.g., toxic level IC_{50}) and concentration threshold sensitivity at least seven orders of magnitude better than existing assays. We anticipate that this technique may serve as the basis for a high-throughput automated screening system that is low-cost, rapid, robust, and informative over a wide concentration range.

PT ASSESSMENT OF THE IMPACT OF γ-RADIATION

The diagnostic value of the PT assay was also used to determine both the "safety limit" of exposure to ionizing γ-radiation (a ^{137}Cs source) and optimal therapeutic doses for cancer treatment [Zharov et al., 2004b]. Studies of the influence of γ-radiation on cancer cells (K562, AR42J, and HepG2) and healthy cells (mouse lymphocytes and RBCs) clearly showed that the

PT technique had the ability to monitor cell-specific responses to radiation that these responses were dose-dependent, and that the characteristic PT response was different for cancerous and noncancerous cells. In particular, the PT assay made it possible to detect the different stages of radiation's impact, from changes in cell metabolism at low radiation doses (0.6–1 Gy) to cell apoptosis at high doses (>1 Gy). The PT assay was also capable of quantitatively differentiating the biological action of γ-radiation on AR42J cells just 20 min after irradiation, whereas the conventional assay showed some apoptosis-related cell response only after 24 h. With the mouse model, the PT assay demonstrated the potential for routine rapid evaluation of the biological consequences to a low dose of radiation in vivo within a few days of exposure, and in particular, increased metabolism shortly after irradiation and inhibition of metabolism in the longer term. Thus, we anticipate that the PT assay has high diagnostic value for evaluating the effects of ionizing γ-radiation on the cellular level that might be important for (1) a highly sensitive in vivo testing of radiation's impact on circulating metastatic and leukemic cells, (2) an innovative biological dosimeter for detecting the effects of radiation within a few days after irradiation and assessing the safety limit of exposure to ionizing γ-radiation, and (3) determining the optimal therapeutic doses for cancer treatment.

It should be noted that in vivo detection of apoptotic cells in blood flow is crucial for understanding the basis of cellular metabolism, as well as the efficacy of antitumor drugs, especially for metastatic cells [Brauer, 2003]. Most existing assays for studying apoptosis are time-consuming and require staining or labeling techniques. In addition, no assay is currently available for detecting apoptosis in flowing cells in vivo. The PTFC assay described above may offer new opportunities to overcome these problems. Because the PT assay is highly sensitive to tiny cellular structures and morphologic changes, it remains the gold standard for recognizing apoptosis [Brauer, 2003]; PTFC could be a promising, if not ideal, tool for detecting apoptosis in vivo.

PT Cell Viability Test

PTFC can be used for highly sensitive monitoring of the penetration of specific absorbing dyes (e.g., trypan blue) into normal and damaged cells in vitro. After laser-induced cell photodamage, a concentration of ~0.01% trypan blue (i.e., ~40 times lower than in conventional cell viability testing) was added to damaged and control cells, which were then analyzed with PTFC in the linear, noninvasive mode. Damaged cells, which accumulated a relatively high concentration of trypan blue, were indicated by the appearance of large PT responses compared to very small PT responses from control cells. Replacement of an absorbing dye with much more strongly absorbing, nontoxic gold PT labels [Zharov et al., 2005d], whose penetration into cells also depends on membrane permeability, should dramatically increase the sensitivity of the PT technique in cell viability testing.

PT Aggregation Immunoassay

PTFC also allowed us to monitor the efficiency of the binding of bioconjugated gold nanoparticles with specific cancer cell markers (e.g., separase) at the single-cell level [Zharov et al., 2005d]. PTFC achieved this by detecting the PT response and red-shift effects as a function of the distances between nanoparticles, their number, and environmental conditions. For in vivo experiments, cells may be targeted with gold nanoparticles having different conjugations. For example, RBCs can be labeled with membrane antigen-specific Abs (e.g., anti-Lewis antibodies), and lymphocytes and neutrophils with CD3-, CD4-, and CD8-specific Abs. Leukemic cells can be conjugated with myeloid-specific Abs as the primary Ab, and can then be incubated with gold nanoparticles conjugated with immunoglobulin G (IgG).

Flow Image Cytometry in Combination With Lymph/Blood Vessels Dynamic Microscopy

Other applications of PTFC in vivo may include determining average cell velocity; RBC deformability in the fast flow of arterioles; the fast-moving (not rolling) portion of WBCs in arterioles and venules; percentage of WBCs experiencing rolling effects (separately for neutrophils and lymphocytes); neutrophil and lymphocyte deformability during adhesion and rolling; cell composition of afferent lymph (e.g., appearance of rare RBCs); and cell behavior in the valve region of lymphatic vessels. Simultaneously, the main parameters of microvessel function can be measured. These parameters include microvessel diameter, parameters of

microlymphatic phasic contractions and valve activity, frequency of lymph flow oscillation, and width of the plasma layer near blood or lymph microvessel walls [Zharov et al., 2005c].

Compared with non-flow PT cytometry, PTFC in vivo is expected to have the advantage of speed—PTFC is at least 100 times faster. And, compared with conventional FC, PTFC also potentially has the advantage of being able to study cells without conventional cell labeling. The detection efficiency (number of cells detected per total number of cells passing through the vessels) is expected to be close to 1 in small lymphatic vessels and blood capillaries using an ellipsoidal beam shape and a beam diameter comparable to that of the vessels. For larger-diameter vessels, we expect to have a problem obtaining a clear PT response from each individual cell. Simultaneous irradiation of several cells with a laser beam is possible, however, if the rare appearance of cells with abnormally strong absorption (e.g., rare RBCs in microlymphatic or gold-labeled cells) is to be determined.

CONCLUSION

While both the PT technique and FC have been available for some time, combining these techniques and using rat mesentery as an animal model is crucial to realizing a new, advanced, integrated PTFC technique that has significant advantages over existing technologies for monitoring circulating cells in vivo. These advantages include (a) noninvasive single-cell diagnostics in the host environment that is not sensitive to scattered light and does not require conventional labeling and scanning; (b) increased absorption sensitivity (at least four orders of magnitude) and improved spatial resolution (up to 300–350 nm); (c) high-speed imaging in fast flow; (d) multiple PT parameters for identifying cells, such as spectrum-dependent PTI and integral PT response; and (e) the potential ability to distinguish various morphologic and functional states of normal and abnormal flowing cells (from metabolic changes to apoptosis and necrosis under normal circumstances and in response to drugs or radiation).

These advantages are important, both for understanding the basic biology of cell metabolism and in vivo cell flow dynamics and for conducting clinical studies of early disease diagnosis or assessment of innovative therapeutic interventions. In cancer research in particular, PTFC has the potential to quantitatively monitor changes in the number of circulating metastatic cells, their interactions with blood and endothelial cells, their accumulation on the endothelium of blood and lymph microvessels and lymph nodes, and their migration through vessel walls. Other potential applications may include radio- and chemosensitivity testing of drugs in vivo and exploration of the possibility of early cancer diagnosis through PT monitoring of small alterations in a cell's absorbing ultrastructure. PTFC has potential to be used in humans; a noninvasive approach might use thin structures, such as an eyelid or interdigital membrane, with optical clearing [Tuchin, 2005], while an invasive approach might involve incorporation of a fiber chip-based catheter in different vessels.

ACKNOWLEDGMENTS

This work was performed at the University of Arkansas for Medical Sciences and supported by the National Institute of Health under Grant EB001858 and in part by the National Institute of Biomedical Imaging and Bioengineering under Grant EB000873 (VPZ is the principal investigator in both grants). The authors thank all colleagues whose results of collaborative work is presented in this review.

REFERENCES

Barber BJ, Oppenheimer J, Zawieja DC, Zimmermann HA. 1987. Variations in rat mesenteric tissue thickness due to microvasculature. Am J Physiol 253:G549–G556.

Becker MD, Planck SR, Crespo S, Garman K, Fleischman RJ, Dullforce P, Seitz GW, Martin TM, Parker DC, Rosenbaum JT. 2003. Immunohistology of antigen-presenting cells in vivo: A novel method for serial observation of fluorescently labeled cells. Invest Ophthalmol Vis Sci 44:2004–2009.

Bornhop DJ, Contag CH, Licha K, Murphy CJ. 2001. Advances in contrast agents, reporters, and detection. J Biomed Opt 6:106–110.

Brauer M. 2003. In vivo monitoring of apoptosis. Prog Neuropsychopharmacol Biol Psychiatry 27:323–331.

Cherry SR. 2004. In vivo molecular and genomic imaging: New challenges for imaging physics. Phys Med Biol 49: R13–48.

Cognet L, Tardin C, Boyer D, Choquet D, Tamarat P, Lounis B. 2003. Single metallic nanoparticles imaging for protein detection in cells. PNAS 100:11350–11355.

Condeelis J, Segall JE. 2003. Intravital imaging of cell movement in tumours. Nat Rev Cancer 3:921–930.

Falvey DE. 1997. Photothermal beam deflection calorimetry in solution photochemistry: Recent progress and future prospects. Photochem Photobiol 65:4–9.

Frazer L. 2000. Go with the flow: An updated tool for detecting molecules. Environ Health Perspect 108:A412–414.

Galanzha EI, Tuchin VV, Zharov VP. 2005. In vivo integrated flow image cytometry and lymph/blood vessels dynamic microscopy. J Biomed Opt 10:54018.

Georgakoudi I, Solban N, Novak J, Rice WL, Wei X, Hasan T, Lin CP. 2004. In vivo flow cytometry: A new method for enumerating circulating cancer cells. Cancer Res 64: 5044–5047.

George TC, Basiji DA, Hall BE, Lynch DH, Ortyn WE, Perry DJ, Seo MJ, Zimmerman CA, Morrissey PJ. 2004. Distinguishing modes of cell death using the ImageStream multispectral imaging flow cytometer. Cytometry A 59:237–245.

Givan AL. 2001. Principles of flow cytometry: An overview. Methods Cell Biol 63:19–50.

Gourley PL, Hendricks JK, McDonald AE, Copeland RG, Barrett KE, Gourley CR, Naviaux RK. 2005. Mitochondrial correlation as a biophotonic marker for detecting cancer in a single cell. Proc SPIE 5699:461–472.

Guck J, Schinkinger S, Lincoln B, Wottawah F, Ebert S, Romeyke M, Lenz D, Erickson HM, Ananthakrishnan R, Mitchell D, Kas J, Ulvick S, Bilby C. 2005. Optical deformability as an inherent cell marker for testing malignant transformation and metastatic competence. Biophys J 88:3689–3698.

Harding CL, Lloyd DR, McFarlane CM, Al-Rubeai M. 2000. Using the microcyte flow cytometer to monitor cell number, viability, and apoptosis in mammalian cell culture. Biotechnol Prog 16:800–802.

Horstick G, Kempf T, Lauterbach M, Ossendorf M, Kopacz L, Heimann A, Lehr HA, Bhakdi S, Meyer J, Kempski O. 2000. Plastic foil technique attenuates inflammation in mesenteric intravital microscopy. J Surg Res 94:28–34.

Jacobs A, Worwood M. 1974. Iron in biochemistry and medicine. London and New York: Academic Press.

Jamin N, Miller L, Moncuit J, Fridman WH, Dumas P, Teillaud JL. 2003. Chemical heterogeneity in cell death: Combined synchrotron IR and fluorescence microscopy studies of single apoptotic and necrotic cells. Biopolymers 72:366–373.

Kim S, Popel AS, Intaglietta M, Johnson PC. 2005. Aggregate formation of erythrocytes in postcapillary venules. Am J Physiol Heart Circ Physiol 288:H584–590.

Kimura H, Sekiguchi K, Kitamori T, Sawada T, Mukaida M. 2001. Assay of spherical cell surface molecules by thermal lens microscopy and its application to blood cell substances. Anal Chem 73:4333–4337.

Kubota F. 2003. Analysis of red cell and platelet morphology using an imaging-combined flow cytometer. Clin Lab Haematol 25:71–76.

Lasch P, Haensch W, Naumann D, Diem M. 2004. Imaging of colorectal adenocarcinoma using FT-IR microspectroscopy and cluster analysis. Biochim Biophys Acta 1688: 176–186.

Lipowsky HH. 2005. Microvascular rheology and hemodynamics. Microcirculation 12:5–15.

Minamitani H, Tsukada K, Sekizuka E, Oshio C. 2003. Optical bioimaging: From living tissue to a single molecule: imaging and functional analysis of blood flow in organic microcirculation. J Pharmacol Sci 93:227–233.

Murakami T, Kobayashi E. 2005. Color-engineered rats and luminescent LacZ imaging: A new platform to visualize biological processes. J Biomed Opt 10:41204.

Nolte MA, Kraal G, Mebius RE. 2004. Effects of fluorescent and nonfluorescent tracing methods on lymphocyte migration in vivo. Cytometry A 61:35–44.

Novak J, Georgakoudi I, Wei X, Prossin A, Lin CP. 2004. In vivo flow cytometer for real-time detection and quantification of circulating cells. Opt Lett 29:77–79.

Oraevsky AA, Karabutov AA. 2003. Optoacoustic Tomography. In: Handbook of biomedical photonics. London: CRC Press. p 34-1–34-34.

Rosenbaum JT, Planck SR, Martin TM, Crane I, Xu H, Forrester JV. 2002. Imaging ocular immune responses by intravital microscopy. Int Rev Immunol 21:255–272.

Sato K, Tokeshi M, Kimura H, Kitamori T. 2001. Determination of carcinoembryonic antigen in human sera by integrated bead-bed immunoassay in a microchip for cancer diagnosis. Anal Chem 73:1213–1218.

Sipkins DA, Wei X, Wu JW, Runnels JM, Cote D, Means TK, Luster AD, Scadden DT, Lin CP. 2005. In vivo imaging of specialized bone marrow endothelial microdomains for tumour engraftment. Nature 435:969–973.

Tamaki E, Sato K, Tokeshi M, Sato K, Aihara M, Kitamori T. 2002. Single-cell analysis via scanning thermal lens mcoroscope with a microchip: Direct monitoring of cytochrome c distribution during apoptosis process. Anal Chem 74:1560–1564.

Tauer U. 2002. Advantages and risks of multiphoton microscopy in physiology. Exp Physiol 87:709–714.

Tibbe AG, de Grooth BG, Greve J, Dolan GJ, Terstappen LW. 2002. Imaging technique implemented in CellTracks system. Cytometry 47:248–255.

Tokeshi M, Uchida M, Hibara A, Sawada T, Kitamori T. 2001. Determination of subyoctomole amounts of nonfluorescent molecules using a thermal lens microscope: Subsingle-molecule determination. Anal Chem 73:2112–2116.

Tozer GM, Ameer-Beg SM, Baker J, Barber PR, Hill SA, Hodgkiss RJ, Locke R, Prise VE, Wilson I, Vojnovic B. 2005. Intravital imaging of tumour vascular networks using multi-photon fluorescence microscopy. Adv Drug Deliv Rev 57:135–152.

Tuchin VV. 2005. Optical immersion as a new tool for controlling the optical properties of tissues and blood. Laser Physics 15:1109–1136.

Wei X, Runnels JM, Lin CP. 2003. Selective uptake of indocyanine green by reticulocytes in circulation. Invest Ophthalmol Vis Sci 44:4489–4496.

Yamamoto N, Jiang P, Yang M, Xu M, Yamauchi K, Tsuchiya H, Tomita K, Wahl GM, Moossa AR, Hoffman RM. 2004. Cellular dynamics visualized in live cells in vitro and in vivo by differential dual-color nuclear-cytoplasmic fluorescent-protein expression. Cancer Res 64:4251–4256.

Zhang JL, Yokoyama S, Ohhashi T. 1997. Inhibitory effects of fluorescein isothiocyanate photoactivation on lymphatic pump activity. Microvasc Res 54:99–107.

Zharov VP. 1986. Laser optoacoustic spectroscopy in chromatography. In: Letokhov VS, editor. Laser analytical spectrochemistry. Boston, Mass: Bristol. p 229–271.

Zharov VP, Lapotko DO. 2005. Photothermal imaging of nanoparticles and cells (review). IEEE J Sel Topics Quant Electron 11:733–751.

Zharov VP, Letokhov VS. 1986. Laser optoacoustic spectroscopy. Berlin: Heidelberg. New York: Springer-Verlag.

Zharov V, Galanzha E, Tuchin V. 2004a. Photothermal imaging of moving cells in lymph and blood flow in vivo animal model. Proc SPIE 5320:185–195.

Zharov V, Galitovsky V, Chowdhuty P, Chambers T. 2004b. Photothermal evaluation of the influence of nicotine, antitumor drugs, and γ- radiation on cellular absorbing structures. Proc SPIE 5329:135–144.

Zharov VP, Galanzha EI, Tuchin VV. 2005a. Integrated photothermal flow cytometry in vivo. J Biomed Opt 10: 51502.

Zharov VP, Galanzha EI, Tuchin VV. 2005b. Photothermal image flow cytometry in vivo. Opt Lett 30:628–630.

Zharov VP, Galitovsky V, Chowdhury P. 2005c. Nanocluster model of photothermal assay: Application for high-sensitive monitoring of nicotine-induced changes in metabolism, apoptosis and necrosis at a cellular Level. J. Biomed 10:44011.

Zharov VP, Kim J-W, Everts M, Curiel DT. 2005d. Self-assembling nanoclusters in living systems: Application for integrated photothermal nanodiagnostics and nanotherapy (review). J Nanomedicine 1: December issue.